Publishing House
AKAPIT

COMPUTER METHODS IN MATERIALS SCIENCE

Informatyka w Technologii Materiałów

Vol. 13, 2013, No. 4

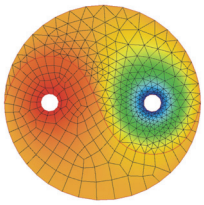

MULTISCALE APPROACH TO MODELLING BLOOD FLOW

ALEKSANDRA JAKUBOWICZ*, MACIEJ PIETRZYK

AGH University of Science and Technology, al. Mickiewicza 30, 30-059 Kraków, Poland
**Corresponding Author: ajakubow@agh.edu.pl*

Abstract

The three dimensional multiscale model is introduced to study clot formation in the vessel with stenosis. The novel approach, based on separation of fluid flow calculation and red blood cells deformation, is proposed. The macro scale fluid dynamic is described by lattice Boltzmann method (LBM). The deformation of red blood cells is calculated by spectrin link method (SLM). The interaction between those two methods is handled by immersed boundary method (IBM). Simulation results demonstrate the structure of the thrombus for three simple geometries.

Key words: blood flow, clotting, lattice Boltzmann method, spectrin link method

1. INTRODUCTION

Blood flow is a very complex process, not only because of the phenomena taking place within the blood itself, but also because of the changes of outer flow parameters. Due to that, the flow pattern can be changed from laminar to turbulent with the geometry changes. The thixotropic nature of the blood allows its coagulation what in consequence prevent bleeding. However, it is possible that thrombus form inside capillaries or devices. This case is extremely dangerous for human health. Therefore, it is important to create a realistic model which concentrates not only on blood flow, but also blood coagulation and fibrinolysis. Approximation of the solution through trial and error method takes time, financial resources and needs experiments on the human body. What is even more important, it does not guarantee a genuine solution of the problem. Computer modelling is an important aid in this case. However, currently available computer programs designed for modelling processes in blood offer a strongly limited description of phenomena occurring in it, focusing mainly on global variables. Additionally, one of the biggest models limitations is the difficulty in verifying and validation of the results. A model of flow through the blood chamber of ventricular assist device (VAD) was developed (Pietrzyk et al., 2012) within the Polish Artificial Heart project (Kustosz et al., 2012). That model was based on the conventional rheological model of blood and was not capable to predict phenomena occurring in the blood microstructure. The present work was planned as an extension of (Pietrzyk et al., 2012) and particular emphasis is on improvement of the micro scale analysis.

The mostly used approach is based on uniform flow assumption. Numerous papers on development and classification of rheological models of blood were published; see for example (Zhang & Kuang, 2000; Yilmaz & Gundogdu, 2008). Primary analysis and classification of rheological models of blood was also performed by the Authors (Szeliga et al., 2009). Mathematical form of various equations was compared and capabilities of the models to account for certain physical features of blood were evaluated. Sensitivity of the viscosity predicted by various models, with respect to the coefficients in these models and with respect to the external variable (shear rate), was determined and importance of the

 ISSN 1641-8581

investigated coefficients and their influence on models predictions was evaluated. This paper is an extension of (Szeliga et al., 2009) and it presents an attempt to apply micro scale modelling techniques.

The VAD has a complex shape, characterized by curvature, bending and tapering. With the addition of valve, a highly complicated three-dimensional flow is obtained. In a diseased environment the flow may become even more complex with the transition to turbulent flow. One of the major drawbacks of mechanically supporting blood flow is the fact that the blood is locally exposed to non-physiological flow conditions, such as high pressures and steep velocity gradients. The blood coagulation followed by thrombus formation is the most dangerous complications, when blood platelets are activated by deformation or contact with air or materials of the implanted device. A risk of coagulation increases if the exposure time is elongated. However, considering only the regions of very low velocities as dangerous is a simplification. Strong turbulences and high shear stresses may induce platelet activation, thus high velocity gradient should be avoided as well. Simplifications base on the assumptions of a rigid material are made. Accurate modelling of these types of flows is crucial for understanding the progress and genesis of cardiovascular diseases.

The objectives of the work were formulated with the above remarks in mind. Various numerical techniques were explored and those advanced methods were selected, which have potential capability to overcome listed above difficulties in modelling of blood flow. Thus, the model presented in this paper does not focus only on the fluid flow problem but it extends obtained results concerning knowledge about processes, which may occur in blood. This is achieved by introducing a multiscale analysis and different numerical techniques at various dimensional scales. In consequence, the model could be used both for simulation of blood flow through large parts, as well as small diameter blood vessels. But what is even more important, this model allows for simultaneous using of different numerical methods.

2. BIOLOGICAL BACKGROUND

The structure of the human heart enables it to function as a mechanical double pump. Vascular disease, which may be present from birth or due to the ageing process, makes the heart unable to provide the required flow rate. Application of VADs may often lead to recovery or, when this is no longer deemed possible, the ventricle will be exploited for bridging until a donor heart becomes available. Modelling of blood flow through the ventricle should support design and exploitation of this device. The objective of this work is exploring possibility of improvement of models, which will help to understand the nature of the blood flow.

The blood performs three major functions in a human body: transport through the body, regulation of bulk equilibrium and body immune defence against foreign bodies. It supplies oxygen, hence energy, conveys nutrients to the tissues and removes carbon dioxide and waste products of cell metabolisms toward lungs and purification organs. The blood includes plasma and solid blood cells. There are three main kinds of cells in blood: erythrocytes (RBC), leukocytes and platelets. Although white blood cells are three times the size of erythrocytes, their role in coagulation model is negligible. Plasma takes approximately 55% of the blood volume and includes the platelets. Activated platelets tend to form blood clots, deactivated platelets do not. The RBC experience reversible deformations during its life span. In its steady state, it has a disc shape with a greater thickness in its outer ring. It is then susceptible to deform when moving with flow. Those deformations are possible by membrane construction, which is essential for development of the spectrin link method. The RBC shape represents an equilibrium configuration that minimizes the curvature energy of a closed surface for given surface area and volume with a geometrical asymmetry. The premature damage of erythrocytes (haemolysis) may lead to a low RBC count and a state of haemolytic anaemia. Apart from low RBC count response, the plasma free haemoglobin is toxic for the kidneys and can eventually lead to multiple organ failure. This is the reason why the erythrocytes deformation is so important to take into account. Mechanical haemolysis starts when an RBC deforms excessively in response to high shearing and it is the dominant mechanism of haemolysis in VADs.

The blood behaves like a concentrated dispersed RBC suspension in plasma. The viscosity of blood depends on the viscosity of the plasma, in combination with the haematocrit, which adds imperfections to the fluid. Increasing of viscosity will lead to decreased of oxygen delivery due to retarded flow. Factors influencing blood viscosity include temperature are not considered in this study. Blood exhibits creep and stress relaxation: if exposed to sinusoidal oscillations reveal a strain-independent loss modulus

and strain-dependent storage modulus. RBCs play a major role on the rheological behaviour of the blood due to both their size and number. The blood exhibits thixotropic behaviour, which is explained by changes in its internal structure, by the kinetics of both reversible RBC aggregation and deformation. Authors presume that computational modelling, if accounts at least for a part of the mentioned features, can provide a useful tool in clinical practice. In the present paper an attempt was made to merge blood flow and cells deformation models in micro scale.

Analysis described in the previous section shows that it is important to understand coagulation process and accompanying phenomena. Even in device which is correctly designed the clotting process will occur. It is mainly because device is not a natural organ and requires anti-clotting medicines to be taken. Blood clots can clog the VAD and keep it from working properly. It should be noticed that, thrombus consist not only clot created in coagulation process but also aggregated platelets on the side of a vessel or device, which are not considered in this work.

The coagulation cascade is complex system of reactions which strengthen the platelet plug. The initial models of coagulation introduced by Davie and Ratnoff (1964) and MacFarlane (1964), see also (Roberts, 2012), are based on cascade or waterfall processes that involve two rather independent pathways, which converge to a common pathway, with thrombin generation as the end point of reactions. These pathways are the contact activation pathway initiated by the exposure to collagen due to minor vessel damages and the tissue factor pathway initiated by the exposure to tissue factor due to vessel rupture. Today it is accepted that these pathways are overlapping and the so-called initiation and propagation phases can be recognized in the kinetics of thrombin generation. Main features of this mechanism are included in the model in the present work. Thus, the model can give the efficient and accurate blood flow simulations. In the domain of medical sciences the results of simulations should provide a better understanding of the coagulation mechanism and should help in design of VAD.

3. MODELS

The objectives of modelling of blood flow can be twofold. The first is prediction of the main flow parameters, such as flow lines, shear rates and shear stresses, turbulence etc. The second is prediction of phenomena occurring in blood due to a flow and due to a contact with walls, including coagulation process. To reach the first objective, in most cases, only one material parameter which is kinematic viscosity has to be known. Relations describing this viscosity as a function of the flow parameters are considered a rheological model of blood. To reach the second objective a micro scale model is proposed.

3.1. Constitutive law

The problem of simulation of blood flow through the artificial heart chamber is governed by typical incompressible flow equations for viscous fluid. The dynamic viscosity coefficient η, which is constant for Newtonian flows, is a function of the shear rate in the case of non-Newtonian flows. The dynamic viscosity coefficient η will be referred to as viscosity in the further part of the paper. The shear rate $\dot{\boldsymbol{\gamma}}$ is written in the following tensorial form:

$$\dot{\boldsymbol{\gamma}} = 2\dot{\mathbf{D}} = \nabla\mathbf{v} + \nabla\mathbf{v}^T \tag{1}$$

where: $\mathbf{v} = \{v_1, v_2, v_3\}$ – velocity vector, $\dot{\boldsymbol{\gamma}}$ - shear rate tensor, $\dot{\mathbf{D}}$ - rate of deformation tensor.

In the case of the generalized non-Newtonian behaviour, the general relation between shear stress tensor $\boldsymbol{\tau}$ and shear rate tensor $\dot{\boldsymbol{\gamma}}$ is:

$$\boldsymbol{\tau} = \eta\left(\dot{\bar{\gamma}}\right)\dot{\boldsymbol{\gamma}} \tag{2}$$

where: $\dot{\bar{\gamma}}$ - effective shear rate tensor, involves the second invariant of the rate of deformation tensor:

$$\dot{\bar{\gamma}} = \sqrt{2\,\mathrm{tr}\,\dot{\mathbf{D}}^2} \tag{3}$$

where: $\dot{\bar{\gamma}}$ - effective shear rate tensor, involves the second invariant of the rate of deformation tensor:

In the present form equation (2) does not account directly for elasticity, stress relaxation or memory effects. Influence of these factors can be accounted for by introduction relevant function in equation (3).

Classification of the rheological models of blood and sensitivity analysis for these models can be found in (Szeliga et al., 2009) and it is not explored further in the present work. More advanced models, which are also discussed, account for the yield stress of blood and its elastic deformation. In some rheological models coefficients are correlated with some physiological and pathological parameters of blood.

The existing models simplify the problem that leads to results, which do not provide comprehensive information about the real phenomena. Available works regarding modelling of blood flow focus on two aspects: first is a description of blood as a homogeneous fluid (e.g. Evans & Skalak, 1980; Dao et al., 2006), second concentrates on red blood cells deformation (e.g. Li et al., 2005; Park et al., 2009). Both approaches have drawbacks, namely, the omission of relevant issues or the nature of the process is not providing full information on the movement. The more advanced model (Boryczko et al., 2004) includes not only red blood cells but also fibrin which is responsible for clotting process. However results are limited to micro and short time scales. These points of view are accurate in only small aspect of wide range of the phenomena occurring during the flow of blood inside VAD. In consequence, this leads to poor quality simulation programs, which are not able to rise to the needs.

3.2. Multiscale model of the blood flow

The overall objective of the work was development of a computer program, which allows for the practical application of the large-scale modelling to solve the problem of incompressible blood flow in three dimensions for both stationary and not stationary processes. Material model is either linear or nonlinear. However, the models must allow for resolving viscosity depending on the history of changes of any parameter of the flow and, consequently, allow for the modelling of thixotropy. Multiscale calculations allows for more accurate calculations in micro scale without the increasing demand for higher processing power. Furthermore, the approach facilitates the modelling of interactions between the phenomena occurring at different scales, providing a comprehensive description of the phenomena in the process. Since blood features are complementary at various scales, the following problems are calculated: homogenous flow by Computational Fluid Dynamics method, red blood cells deformation by solid mechanics and blood coagulation process.

The conventional rheological models are not well amenable for capturing phenomena occurring in micro scale in blood. Accordingly to multi-physics phenomena and multi scale analysis, the proper capturing of these phenomena is the major challenge in contemporary computational fluid mechanics. The methods allowing coping with those challenges are usually classified into two groups: upscaling methods and concurrent multiscale computing (Allix, 2006; Madej et al., 2008). The former approach is used in the present work.

In the upscaling class of methods constitutive models at higher scales are constructed from observations and models at lower, more elementary scales. By a sophisticated interaction between experimental observations at different scales and numerical solutions of constitutive models at increasingly larger scales, physically based models and their parameters can be derived at the macro scale. The methods of computational homogenization are considered to belong to this group of methods.

The idea of micro scale model is presented in figure 1. Each module represents separate procedure. Because calculations concentrate only on blood flow and erythrocytes deformation, the coagulation process required additional procedure described below. An illustration of this pattern is a description of the various methods and interactions between them. The individual subroutines at run time are not dependent one on another, in a straightforward manner. Information transmitted between the scales provides input parameters and output routines only. Thus, it is possible to adapt the model to realistically describe the phenomenon by changing any of the methods.

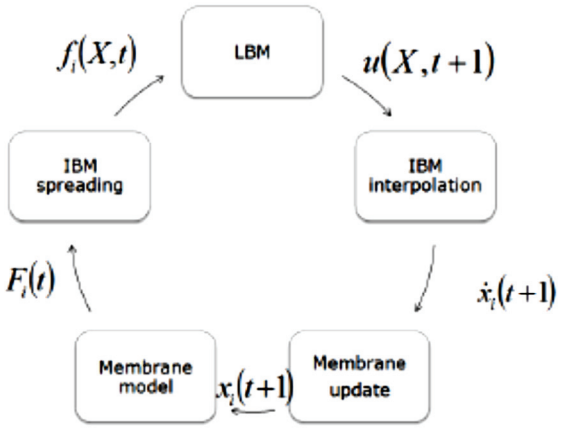

Fig. 1. *Schematic diagram of the micro scale model.*

The algorithm able to simulate micro level RBCs flow can be summarized as follows:

1. Obtain the new velocity field v(x, t+1) (LBM).
2. Interpolate the fluid velocity back to the fluid nodes and obtain $\dot{x}$ (t+1) (IBM).
3. Update all node positions according to $x_i(t+1) = x_i(t) + \dot{x}_i\ (t+1)$.
4. Compute the membrane forces $F_i(t)$ based on the membrane deformation model (SLM).
5. Spread the forces to the lattice and obtain the lattice force density (IBM).

6. Go back to step 1.

There are the three important state variables: the field of shear rate, haematocrit and degree of agglomeration. These parameters are determined and modified based on the results of simulations. Velocity field is determined using the lattice Boltzmann method. The velocity of the fluid on the boundary, determined by the immersed boundary method, defines the velocity of the point on the RBC membrane. Base on this information the new position is calculated. Then the deformation model calculates forces acting on the membrane. The more detailed description of used methods will be provided below.

3.3. The lattice Boltzmann method

The lattice Boltzmann method was selected due to a small computational power required and no need for remeshing. This method is based on the microscopic kinetic equation for the particle distribution function $f_i(x,t)$, which can be described as probability of finding a molecule at a position x, travelling with velocity v in direction e_i, at time t. The physical space is described by regular grid, in which the directions of possible movements are defined. The most popular D3Q19 model was used (three dimensional and contains nineteen velocities). These velocities are either 0 or ±1 in directions at the physical position. Unlike the molecular dynamic method, the populations are not separated but each of them influences the distribution function.

In this method the discrete Boltzmann equation is solved instead of the Navier-Stokes (N-S) equations. Base on the continuous Boltzmann equation the lattice Boltzmann equations can be derived:

$$\frac{\partial f(x,v,t)}{\partial t} + v\nabla_x f(x,v,t) = \left(\frac{\partial f}{\partial t}_{col}\right) \qquad (4)$$

where: t - time, x - position, v - velocity, $\left(\frac{\partial f}{\partial t}\right)_{col}$ - collision term.

Collision is described by a single relaxation time approach proposed by Bhatnagaret al. (1954). In this approach the distribution function aims at the equilibrium state, which is thermodynamic equilibrium described by Maxwell-Boltzmann distribution:

$$\left(\frac{\partial f}{\partial t}\right)_{col} \approx -\frac{f - f^{eq}}{\tau} \qquad (5)$$

By using this approach a discretized transport function is obtained:

$$\underbrace{f_{i+1} = f_i}_{streaming\ term} \underbrace{- \frac{f_i - f^{eq}}{\tau}}_{collision\ term} \qquad (6)$$

Developing f_i^{eq} into a power series with an accuracy of the second order in the low speed range, we will obtain equilibrium:

$$f_i^{eq} = \rho\omega_i\left[1 + 3e_i u + \frac{9}{2}(e_i u)^2 - \frac{3}{2}u^2\right] \qquad (7)$$

where: ω_i - the values of weights to ensure isotropy.

For D3Q19 model these weights are ω_0 =1/3, $\omega_{1\ldots6}$ =1/18,$\omega_{7\ldots18}$ =1/36. By using the Chapman-Enskog expansion, equation (4) can recover the N-S equation to the second order of accuracy. Two subsequent steps are repeated over the duration of the simulation: streaming and collision. The first considers only movement in specific direction to the nearest neighbour lattice node. The second is considered as a relaxation towards a local equilibrium.

Such macroscopic values as density and velocity are related to the sum of local distribution functions:

$$\rho = \sum f_i \qquad \rho v = \sum f_i e_i \qquad (8)$$

To ensure accuracy and stability it is needed to define appropriate boundary conditions. The following boundary conditions are used:

- Periodical boundary conditions, where distribution function coming out of one boundary, enters into the opposite boundary. Those conditions are then applied directly to the distribution function. In our test they are applied to inlet and outlet sections of the capillary for RBCs.
- Bounce back boundary condition, where distribution function coming out of one boundary is reflected. This condition (full way bounce-back) leads to mass and momentum conservation, but it gives only first order numerical accuracy, which means the lowest-order term in the truncation error is first order. There exist several variants of this method trying to improve it. These methods are mentioned below, due to possibility of defining interface between the two phases. The second order accuracy in space could be obtained by using the halfway bounce-back scheme. In this scheme the wall is placed at halfway between a fluid node and a bounce-back node. Those conditions were applied to capillary wall.

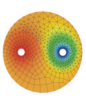

3.4. The spectrin link method

RBC deformation depends on its membrane which consists of a lipid bilayer to which a spectrin network is attached. That makes it tough and flexible. The spectrin form two-dimensional mesh. Basic length of spectrin is 200 nm, which cross links the vertexes. The average length between two vertexes is 75-80 nm (Liu et al., 1987). In the spectrin link model each RBC membrane can be approximated by a network of points x_n, $n \in N$, which are the vertices of the erythrocytes surface triangulation and are defined in Cartesian three dimensional system.

In this method deformation of single RBC depend on minimization of membrane Helmholtz energy:

$$Ex_n = E_{in-plane} + E_{bending} + E_{volume} + E_{area} \quad (9)$$

The in-plane contribution is expressed in two terms as:

$$E_{in-plane} = \sum_{i \in spectrin\ links} V_{WLC}(L_i) + \sum_{\alpha \in triangle\ palaquetts} \frac{C_q}{A_\alpha} \quad (10)$$

Where L_i - the length of spectrin link i and A_α - the area of triangular plaquette α. The first summation includes all spectrin links and can be defined as the total entropic free energy stored in the spectrin proteins described in terms of the worm-like chain (WLC).The force-length relationship is rooted in DNA mechanics and for this particular case is modelled by:

$$V_{WLC}(L_i) = \frac{k_b T L_{\max}}{4p} \frac{3x^2 - 2x^2}{1-x} \quad (11)$$

where: $L_{\max}$ - the maximum or contour length of the chain, p - the persistence length, k_B - the Boltzmann constant, T - the temperature in K.

The second summation is the hydrostatic elastic energy stored in the lipid membrane and other protein molecules. Constant C_q and exponent q have to be selected.

The bending contribution takes into account the angle between adjacent pairs of triangles that describe the RBC membrane:

$$E_{bending} = \sum_{\alpha\beta\, pair} k_{bend}[1 - cos(\theta_{\alpha\beta} - \theta_0)] \quad (12)$$

where: $\theta_{\alpha\beta}$ - the instantaneous angle, θ_0 - the initial angle between adjacent triangles. The numerical treatment of these angles is given in more detail in (Liet et al., 2005).

The constraint on the volume ensures that the volume of the RBC enclosed by the triangulated membrane remains constant:

$$E_{volume} = \frac{k_{volume}(\Omega_{total} - \Omega_{total}^{desired})^2}{2L_0^3 \Omega_{total}^{desired}} \quad (13)$$

where: Ω_{total} - the instantaneous volume area of the RBC, $\Omega_{total}^{desired}$ - the initial or desired volume of the erythrocytes. This is also enforced due to the incompressible nature of the fluid within each RBC governed by the LB method.

The constraint on area takes a form similar to that of the volume and serves to conserve the surface area of the RBC:

$$E_{area} = \frac{k_{area}^{global}\left(A_{total} - A_{total}^{desired}\right)^2}{2L_0^2 A_{total}^{desired}} + \sum_{\alpha \in \Pi} \frac{k_{area}^{local}\left(A_\alpha - A_\alpha^0\right)^2}{2L_0^2 A_\alpha^0} \quad (14)$$

where: A_{total} - the instantaneous surface area of the RBC, $A_{total}^{desired}$ - the initial or desired area of the erythrocytes, A_α^0 - the instantaneous area of triangle. The first term of the area equation contributes to the global area conservation while the second term contributes to the local area conservation. The area constants k_{area} are typically chosen such that the local contribution is much smaller than the global contribution.

When using methods such as particles dynamics the choice of k parameters is dependent on Boltzmann constant and temperature, but since the LB method is independent of temperature, these constants are arbitrary and are chosen to match non-dimensional parameters of interest.

Under physiological conditions, it is assumed that normal human erythrocytes in an unstressed state are represented by a biconcave discus shape (figure 2):

$$z = R\sqrt{1 - \frac{\left(x^2 + y^2\right)}{R^2}}\left[c_0 + c_1 \frac{\left(x^2 + y^2\right)}{R^2} + c_2 \frac{\left(x^2 + y^2\right)^2}{R^4}\right] \quad (15)$$

where: R = 6 μm, c_0 = 0.1035805, c_1 = 1.00127, c_2 = -0.561381.

A parametric representation for the red blood cells allows us to accurately perform the required operations and effectively handle changes in the cells morphology such as elongation and swelling. The shape of membrane depends on membrane

model calculations. The initial cell mesh is created once for all cells due to the energy criteria. Then a cell is probabilistically positioned in the blood volume to enable the simulation.

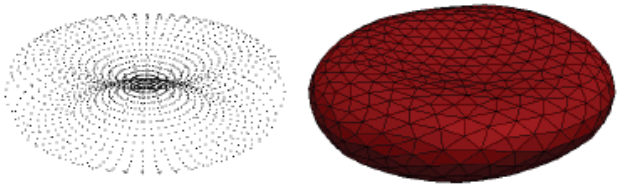

Fig. 2. *Formation of initial red blood cell membrane. Left: initial points distribution (N = 1924 points). Right: coarse-grained model (N = 500 points).*

3.5. The immersed boundary method

The immersed boundary method was used to create the interface between fluid and RBCs. It is based on introducing two calculation meshes: the Eulerian grid for the fluid (stationary and regular) and Lagrangian mesh for the boundaries (generally non-stationary and unstructured). The suspended particles move continuously in space while the no-slip boundary condition on the surface of the particle is satisfied by the requirement that the fluid velocity at the solid boundary node is equal to the solid velocity at that point. For the immersed boundary method, the effect of boundary is represented by a set of force density (force per volume), which acts on the fluid field surrounding the boundary. There is no direct boundary condition for the fluid (especially not for the distribution function). This means that the populations can cross the boundaries without seeing them, but the macroscopic fluid behaves as if there was a boundary. Additionally, the fluid fills the entire space, even inside the boundary region.

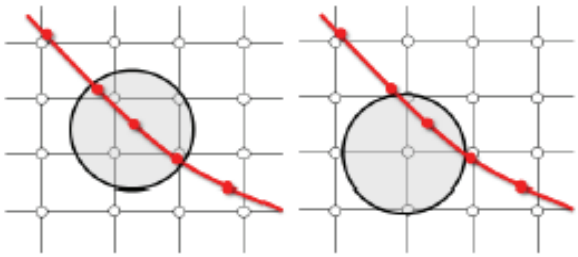

Fig. 3. *Illustration of velocity interpolation (left) and force spreading (right).*

In the IBM, at every evolution time step, if the velocity of fluid at the boundary point is equal to the velocity of boundary at the same position, the non-slip boundary condition would be strictly guaranteed. But the fluid velocity is known only at grid nodes and has to be interpolated to arbitrary points. The basic idea is that all forces, which act on the boundary, also have to act on the ambient fluid in order to ensure total momentum conservation. A sketch of the interpolation and spreading operations is shown in figure 3.

In the IBM-LBM boundary condition, the fluid velocities at the boundary points are enforced to be equal to the boundary velocities, which would produce a set of velocity corrections at these points. The force located at the immersed boundary node affects the nearby fluid mesh nodes through a discrete version of the Dirac delta distribution function:

$$f\left(X,t\right)=\sum_{i}F_{i}\left(X,t+1\right)\Delta\left[x_{i}\left(t\right)-X\right] \quad (16)$$

where: F_i - force acting on node i.

The movement of the immersed boundary node is also affected by surroundings fluid movement:

$$\dot{x}\left(t+1\right)=\sum_{X}u\left(X,t+1\right)\Delta\left[x_{i}\left(t\right)-X\right] \quad (17)$$

where: $x_i(t)$ - position of the boundary node i, $u(X,t)$ - fluid velocity.

It is not directly obvious, which function to select as the interpolation function in order to approximate Dirac delta distribution. The procedure to find suitable functions is described by Peskin (2002). The following model was used in the present paper:

$$\Delta(x)=\begin{cases}1-\|x\|, & 0\le\|x\|\le 1\\ 0, & 1<\|x\|\end{cases} \quad (18)$$

where: x – position of the membrane node.

To provide the best method efficiency the size of meshes should be comparable. Since the simplest Delta function model was used, the numerical precision can be improved. However, it is possible to reproduce the real RBC motion and the method is high efficient. The immersed boundary method makes possible to take into account history of the RBCs deformation.

3.6. Clotting model

The clotting process is complicated and its complex description needs high computational power. The model based on age criteria is used in this paper. The age of fluid is defined by time step in which the fluid (plasma) entered the domain. The clotting may occur when certain threshold of fluid age is reached. The coagulation process causes increase of viscosity

till the maximal stable value. In this case it is implemented as a decrease of the collision frequency to its minimal stable value. When the threshold is reached the solidification process occurs. A cell which fulfils this condition changes state to a clot. In the LBM, due to lack of mesh there is no need for remeshing like in classical methods. During following time steps for the corresponding cells there are still calculations but because of high viscosity there fluid velocity is low. However, if flow condition would change there would be possibility for size reduction of created clot. Yet, to simulate more realistic phenomena additional conditions need to be taken into account. Only when solidification would occur at a wall of vessel the clot could attach itself to it. That means the clot cannot be created inside fluid flow. It is accomplished by extra condition which says that cell can form clot only if at least one of neighbouring cells is boundary one or clot already. The second limitation exists because of shear stress criteria. The clot can be formed only when shear stress is below the shear stress threshold. The simulation parameters (clotting age, limiting shear stress threshold) were chosen that clotting occurs in the desired regions.

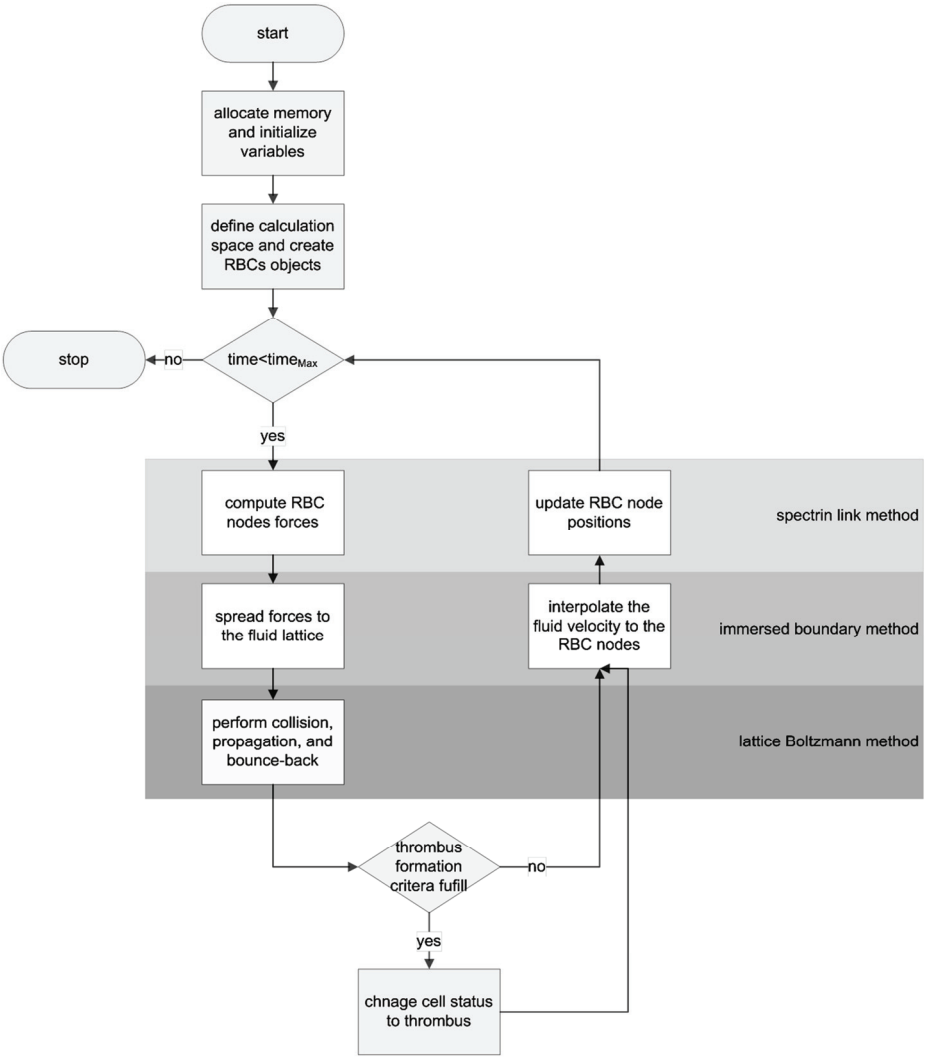

Fig. 4. Schematic diagram of the program.

4. ALGORITHM AND COMPUTER PROGRAM

Based on the description from chapter 3, the multiscale model was created (figure 4). Before the actual simulation starts program is initialized. This includes allocation of needed memory, as well as, a loading of simulation geometry. The initial RBCs distribution is created randomly. The main program loop, which is repeated in each time step, consists 6 steps. The first step is computation of particles forces in each of membrane nodes for each of erythrocytes. Then the forces are spread from Lagragian to Eulerian mesh according to IBM rules. The next simulation step is LBM (the collision, propagation and bounce back is preformed). In this step fluid parameters are calculated. The macroscopic quantities like density and velocity can be extrapolated. In next step fluid velocities are interpolated on membrane nodes. Then a particle position is updated. After simulation of fluid and RBCs motion, the thrombus formation procedure is launch. Cells, where all of the clot formation criteria are fulfilled, change state to clot. Then procedure is repeated till defined time criteria.

5. NUMERICAL TESTS

Based on the previous research on blood flow through VAD it is seen that micro scale simulations are significant for quality of obtained results. Because of it in this paper we concentrate on micro level simulations rather than whole part. All tests were conducted for three dimensional cases but figures show the two-dimensional slice planes. Numerical tests were performed to validate the model and

to evaluate its robustness. The first one focuses on modelling of BRCs deformations where second one investigates a clot formation problem.

5.1. RBC deformation

For the first case two tests were conducted: fist one with only one RBC to validate accuracy of program, second one with multiple cells flow. Single RBC suspended in a linear shear flow with different shear rate was considered. The linear shear flow field was obtained by adding the velocity boundary condition at the bottom and top. The computation domain was $\phi 30 \times 30$. It is seen in figure 5 that the typical erythrocytes motions observed in experiments and simulations can be reproduced. At the low shear rate (50 s^{-1}), the RBC makes tumbling motion. At the higher shear rate (500 s^{-1}) cells perform a tank-treading motion. The velocity field (figure 6) demonstrates that the inner fluid of the cell undergoes a rotational flow, which is induced by the cell membrane tank treading. At the same time the membrane, although the global shape of the erythrocytes is stationary, is rotating along the vesicle with a constant velocity and steady inclination angle. Swinging is obtained at the shear rate of a transition value (150 s^{-1}). Because a single RBC suspended in a linear shear flow simulations give a reliable results the multiple RBC motion will be investigated. The simulations of RBCs in a flow through channel were made for initial distribution of cells presented in figure 7. The flow is from left to right. The computation domain was $\phi 30 \times 130$.The haematocrit level was 40%. The pressure gradient was set along vessel with the periodic boundary condition for erythrocytes at the inflow and outflow boundaries. The simulations were conducted for three values of maximum pressure. The behaviour of the same RBCs were considered for all cases. The velocities distributions in lattice units are presented in figures 8, 9 and 10. The v_{max} is the maximal velocity according to initial conditions. The results not show the steady state but the evolution of solution. It is seen that the simulation proceeds in a similar way depending on

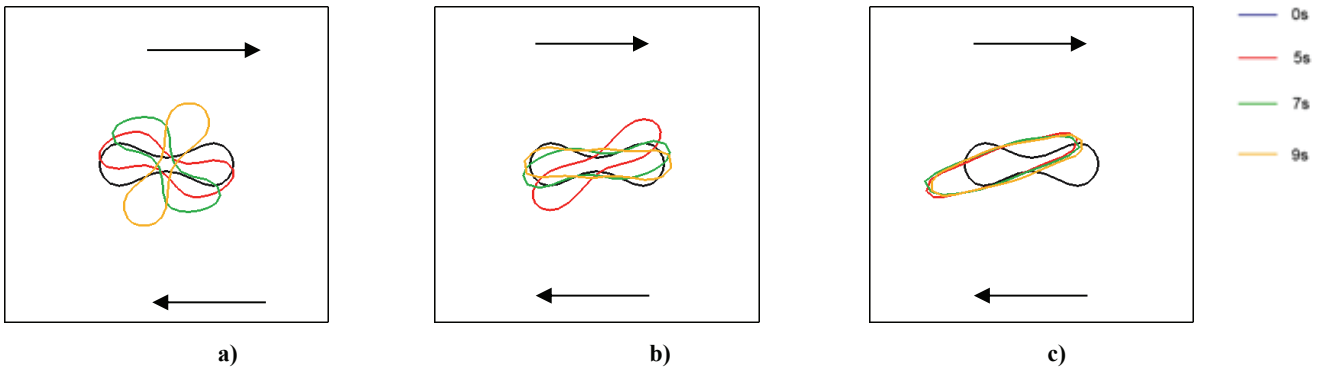

Fig. 5. Motions of RBC in shear flow: a) tumbling motion at a shear rate γ of 50 s−1, b) swing motion at a shear rate of 150 s^{-1}, c) tank-treading motion at a shear rate of 500 s^{-1}.

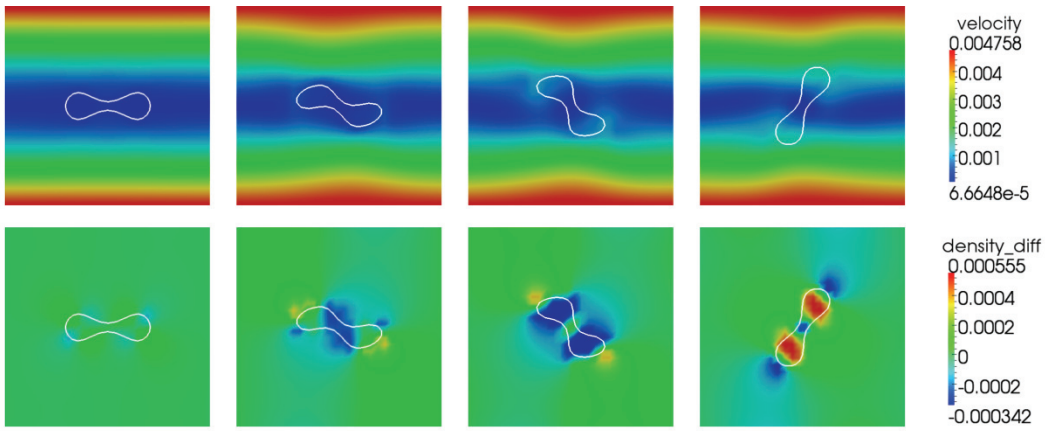

Fig. 6. Velocity field (top) and density difference field (bottom) during tank-treading motion of a vesicle in a shear flow (times steps: 0, 5, 7, 9 s).

the maximum value. The cells are mainly influenced by the viscous force and the shape change is large. With increase of maximal velocity the deformation of erythrocytes is also increasing. It has been found that the RBC exhibits parachute shape with the curvature closely related to the deformability of the cell membrane and the haematocrit of the blood, and can recover its initial shape associated with the minimal elastic energy when the flow stops. If the RBC is initially perpendicular to the incoming flow direction, it gradually changes the geometric shape from a biconcave to a parachute shape, with the curvature closely related to the deformability of the cell membrane. Similarly, the deformation and the restoration are observed when the initial orientation of the RBC is changed. It is also seen that RBCs which are close to vessel wall have elongated shape due to higher shear stresses which are acting on them. At higher speed the Fåhræus effect is earlier visible - erythrocytes move over the centre of the vessel.

5.2. Thrombus formation

The three-dimension pipe with stenosis was investigated for the coagulation test. Three different sets of stenosis were placed inside the vessels. Figure 11 shows the two-dimensional slice planes of the three geometries to demonstrate the placement and sizes of the stenosis. First geometry is a single stenosis within the vessel. The diameter of the stenosis is as large as the length; the diameter of the pipe is 1.5 times as large. The second geometry is three times longer. Third one is multiple stenosis with size like a single one. The diameter of the vessel is 30 mm, length is 200 mm.

In figure 12 the clot simulation is marked with red colour. It can be seen that a small clot forms in front of the stenosis (within the small recirculation region) and a larger clot forms after the stenosis, where a large recirculation region occurs. The velocity increases at the beginning of the stenosis due to the reduction of the diameter, but after its end it does not drop (it is cause by lack of recirculation regions).

Similarly as in the case of a single short stenosis, the larger clot is formed after it (figure 13). However, the clotting size is bigger this time. It is connected with fluid clot criteria. When the age is higher the clot can fulfil criteria easier. Figures 13 shows the analogues velocity distribution like in previous case.

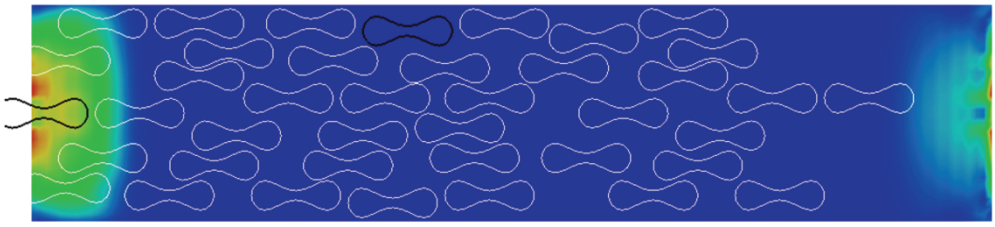

Fig. 7. *The initial distribution for RBCs.*

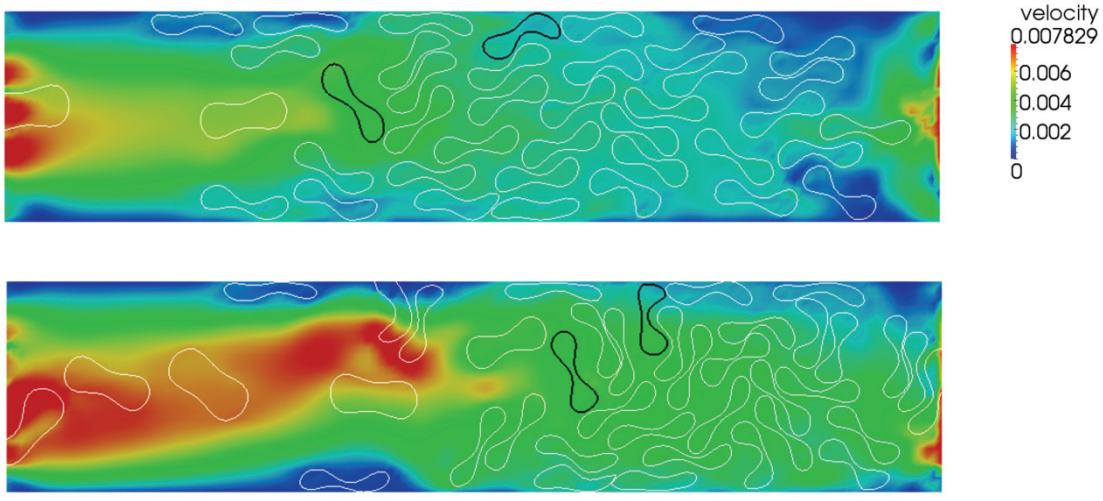

Fig. 8. *Snapshots of RBCs behaviour in a flow for v_{max} = 0.08 (for times steps: 4 and 8 s).*

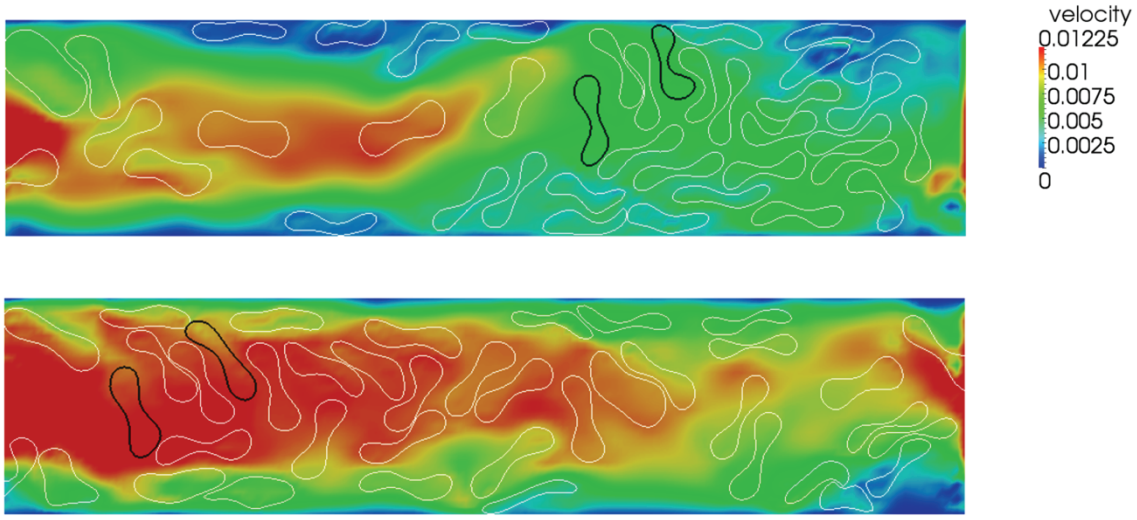

Fig. 9. *Snapshots of RBCs behaviour in a flow for v_{max} = 0.12 (for times steps: 4 and 8 s).*

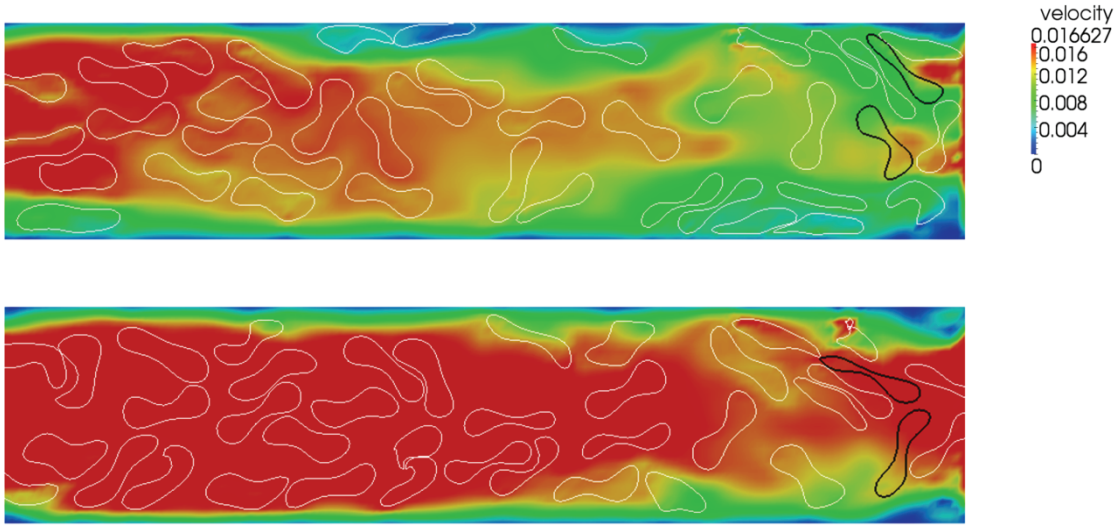

Fig. 10. *Snapshots of RBCs behaviour in a flow for v_{max} = 0.16 (for times steps: 4 and 8 s).*

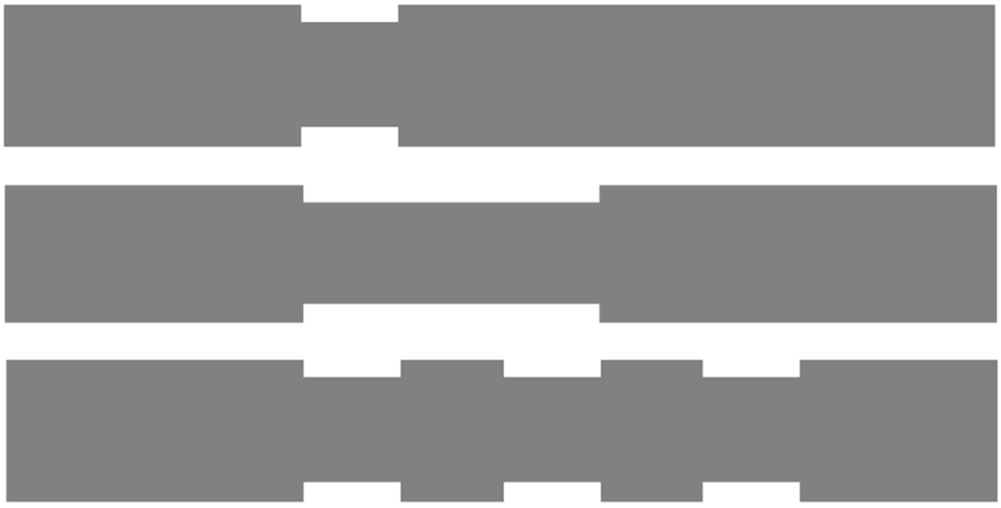

Fig. 11. *The shape of the vessel for clot formation investigation.*

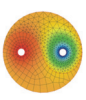

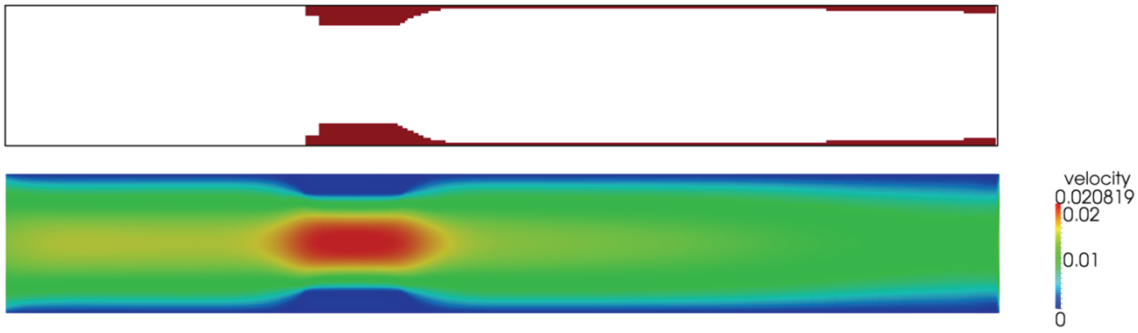

Fig. 12. *The shape of the clot and velocity distribution for a single short stenosis.*

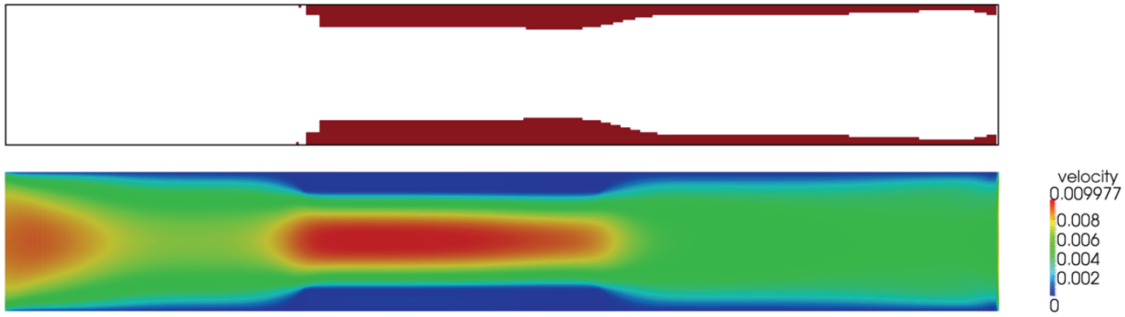

Fig. 13. *The shape of the clot and velocity distribution for a single long stenosis.*

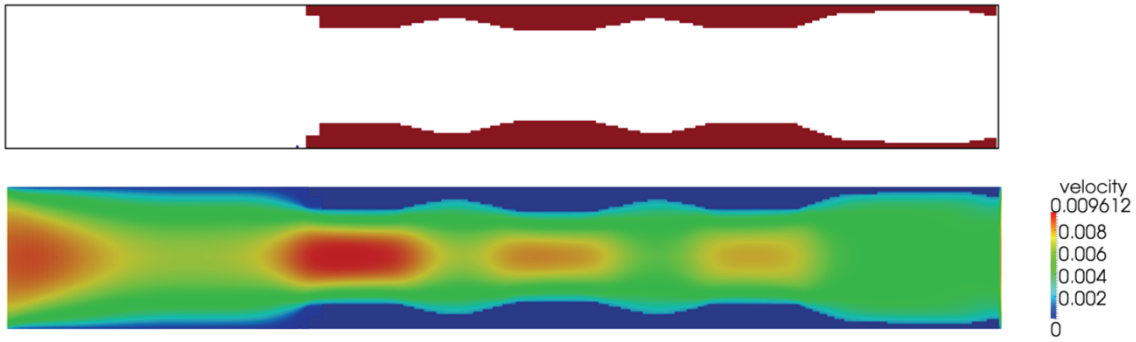

Fig. 14. *The shape of clot and velocity distribution for triple stenosis.*

Figure 14 shows clot before and after stenosis region similar to the presented earlier test cases. The reduction of diameter between stenosis is caused by clot formation. The velocity distribution is similar to other test cases. The choice of critical values is significant for the clot formation. The low threshold value increases the size of the clot, but to high values would lead to unrealistic results.

6. CONCLUSIONS

A novel multiscale approach was proposed is this paper. The basic construction and methods of the model were presented. It was shown that the lattice Boltzmann method can be successfully used for blood flow simulation. This method represents a viable alternative to the Navier Stokes solvers with low need of computational power. The spectrin link membrane method allows predicting red blood deformation with satisfactory qualitative accuracy. Because of cell aggregation process the parabolic profile of the flow is disturbed. This process is better pronounced at low speed due to the applied shear stresses.

Used simple clotting model based on age criteria gave a reasonably good results. The results demonstrate that the velocity of the blood flow in stenotic channel is decreased by the stenoses. The thrombus forms in expected regions: within recirculation regions which occur in front of the stenosis and the most important behind the stenosis. The actual form and size of the clot forming is mostly dependent on the choice of the shear stress limitation. However, further restrictions are needed for obtaining more realistic results. Without other criteria the very long pipe would be clotted due to the time required by the

fluid to travel to this location. Investigation of the influence of a pulsating flow condition on the formation of the clot will be the topic of the further work. It would be significant to include platelets in system to obtain more realistic model.

By using presented model it is possible to investigate not only the heterogeneous blood flow but also the RBCs deformation and clot formation related to it. In the single simulation it is possible to focus study on a selected process but, what is more important, it is also achievable to examine how particular processes depend on each other. In consequence, the application to VADs simulation would be straightforward and benefit of it would be obvious (knowledge about the mechanical haemolysis and thrombus location). The further works are planned in this area, as well as the comparison with real clot form and size.

It should be emphasized that this is the primary version of the model. Further works would concentrate on the sensitivity analysis, identification of the model parameters and validation by comparison with the experimental results.

REFERENCES

Allix, O., 2006, Multiscale strategy for solving industrial problems, *Computational Methods in Applied Science*, 6, 107-126.

Boryczko, K., Dzwinel, W., Yuen, D.A., 2004, Modeling fibrin aggregation in blood flow with discrete-particles, *Computer Methods and Programs in Biomedicine,*75, 181-194.

Bhatnagar, P.L., Gross, E.P., Krook, M., 1954, A model for collision processes in gases. I. Small amplitude processes in charged and neutral one-component systems, *Physical Review,* 94, 511-525.

Dao, M., Li, J., Suresh, S., 2006, Molecularly based analysis of deformation of spectrin network and human erythrocyte, *Materials Science and Engineering C*, 26, 1232-1244.

Davie, E.W., Ratnoff, O.D., 1964, Waterfall sequence for intrinsic coagulation, *Science*, 145, 1310-1312.

Evans, E.A., Skalak, R., 1980, *Mechanics and thermal dynamics of biomembranes*, CRC Press, Boca Raton.

Kustosz, R., Gonsior, M., Jarosz, A., (eds), 2012, *Technologie inżynierii materiałowej i technologie metrologiczne dla potrzeb polskich protez serca*, FRK Zabrze (in Polish).

Li, J., Dao, M., Lim, C.T., Suresh, S., 2005,Spectrin-level modeling of the cytoskeleton and optical tweezers stretching of the erythrocyte, *Biophysical Journal*, 88, 3707-3719.

Park, J.S., Song, S.H., Jung, H.J., 2009, Continuous focusing of microparticles using inertial lift force and vorticity via multi-orifice micro fluidic channels, *Lab on a Chip*, 9, 939-948.

Pietrzyk, M., Banaś, K., Milenin, A., Kopernik, M., Szeliga, D., Macioł, P., Cybułka, P., Michalik, K., 2012, Model numeryczny sztucznej komory wspomagania pracy serca, in: *Technologie inżynierii materiałowej i technologie metrologiczne dla potrzeb polskich protez serca*, eds, Kustosz, R., Gonsior, M., Jarosz, A., 373-439 (in Polish).

Peskin C.S., 2002, The immersed boundary method, *Acta Numerica*, 11, 479-517.

Roberts, H.R., 2012, Oscar Ratnoff: his contributions to the golden era of coagulation research, *British Journal of Heatomology*, 122, 180-192.

Szeliga, D., Kopernik, M., Pietrzyk, M., 2009, Critical evaluation and sensitivity analysis of rheological models of human blood, *Computer Methods in Materials Science*, 9, 435-450.

Yilmaz, F., Gundogdu, M.Y., 2008, A critical review on blood flow in large arteries; relevance to blood rheology, viscosity models, and physiologic conditions, *Korea-Australia Rheology Journal*, 10, 197-211.

Zhang, J.-B., Kuang, Z.-B., 2000, Study on blood constitutive parameters in different blood constitutive equations, *Journal of Biomechanics*, 33, 355-360.

WIELOSKALOWE PODEJŚCIE DO MODELOWANIA PRZEPŁYWU KRWI

Streszczenie

W artykule przedstawiony jest trójwymiarowy wieloskalowy model mający na celu modelowanie tworzenia się skrzepu w naczyniu krwionośnym ze zwężeniem. Zaproponowane nowatorskie podejście, oparte jest na rozdzieleniu obliczeń przepływu płynu i odkształceń krwinek czerwonych. Poziom makro przepływu krwi jest obliczony za pomocą metody siatkowej Boltzmann (ang. lattice Boltzmann method). Deformacja krwinek czerwonych opisana jest przez metodę powiązań spektryny (ang. spectrin link method).Interakcje między tymi dwoma metodami są możliwe dzięki metodzie zanurzonej ścianki (ang. immersed boundary method). Wyniki symulacji przedstawiają kształt skrzepu dla trzech prostych geometrii.

Received: November 3, 2013
Received in a revised form: November 28, 2013
Accepted: December 11, 2013